

Theoretical study of the spin-polarized Auger-electron emission from K caused by circularly polarized light

Yu. Kucherenko

Institute of Metal Physics, National Academy of Science of Ukraine, 252142 Kiev, Ukraine

P. Rennert*

Physics Department, Martin-Luther-University Halle-Wittenberg, D-06099 Halle, Germany

(Received 15 January 1998)

The calculations of the spin-polarized K $M_{2,3}VV$ (where VV is valence-valence) Auger-electron emission following a core-hole excitation by polarized photons from the potassium surface has been performed. The spin polarization of the K $M_{2,3}VV$ Auger electrons depends on the energy of the incident circularly polarized radiation due to the mixing of s and d waves in the photoelectron final states. Furthermore, it has been shown that taking into account the different orbital symmetry of the valence electrons in the screening cloud can affect significantly the value of the Auger-electron spin polarization. The quantitative agreement of the calculated results with the experiment has been achieved. The connection between photoelectron, core-hole, and Auger-electron spin polarization, respectively, is discussed. It has been shown that these quantities can have quite different values. Whereas the photoelectron spin polarization can be simply expressed in terms of the core-hole spin polarization, the Auger-electron spin polarization may even have equal or opposite sign as compared to the core-hole one. [S0163-1829(98)05531-3]

I. INTRODUCTION

It is well known that Auger electron spectroscopy provides information on the characteristics of chemical bonds and the electronic structures of solids.^{1,2} Recently the development of the angle-resolved and spin-resolved spectroscopic techniques makes it possible to perform more detailed investigations of the spatial and energy distribution of the electronic states as well as their symmetry characterization.^{3,4} It has been shown⁵ that spin-polarized Auger-electron spectroscopy is a powerful probe of local magnetic properties of solids, and it has been successfully applied to the study of ferromagnetic materials.⁶⁻⁹ However, if the circularly polarized radiation is used for the excitation of the Auger process, the primary core hole has a preferred spin orientation. As a result, one obtains the spin-polarized Auger emission also from nonmagnetic materials. This could be an additional source of information on electronic states in solids.

In Refs. 10 and 11 the spin-dependent core-valence-valence (CVV) Auger decay in alkali metals has been studied. It has been shown that the measured Auger-electron spin polarization correlates with the symmetry of the unoccupied conduction band reached in the primary photoexcitation. The obtained experimental results have been interpreted qualitatively using an atomic model and Auger transition selection rules. This simple model describes the behavior of the Auger-electron spin polarization with increasing energy of incident photons, but predicts considerably higher values for spin polarization than the measured ones.

We have performed the theoretical study of the spin-polarized Auger-electron emission from the potassium surface excited by circularly polarized radiation. The aim of our work is to remove the discrepancies between theory and experiment taking into account effects that have not been in-

cluded in the simple atomic model. These are spin-dependent Auger matrix elements, local valence-band structure in the presence of the core hole, and diffraction of the outgoing Auger wave on the atoms of the crystal.

In Sec. II we describe the theoretical model used for calculations. In the following sections we analyze in detail the process of formation of the K $M_{2,3}VV$ Auger spectra for various levels of approximations used in the theoretical model. In Sec. III we discuss the connection between photoelectron, core-hole, and Auger-electron spin polarization, respectively. In Sec. IV we discuss the results provided by the atomic model,¹⁰ taking into account, however, Auger transition matrix elements. Finally, in Sec. V the calculated local valence-band structure for potassium crystal is considered for the K atom in the ground state as well as for the K atom having a $3p$ core hole and the role of the valence-band states having different symmetry in the formation of the shape of the Auger spectra is shown. This step-by-step consideration of the Auger-electron emission give us an opportunity to separate the processes that contribute to the formation of the Auger-electron flux and determine its intensity and spin polarization. Conclusions are drawn in Sec. VI.

II. BASIC EQUATIONS AND DETAILS OF CALCULATIONS

The theoretical model and the main approximations used for the description of the Auger process have been given in Refs. 12 and 13. Here we present the general expressions used for the calculation of the spin-polarized Auger-electron intensity.

We assume the CVV Auger process to be a three-step process. These steps are the following: (i) an atom in the solid is excited by the incident photon and the core-hole state is created; (ii) Auger decay of the core hole, which is filled

by an electron from the occupied valence band while another valence electron is lifted into an unoccupied state; and (iii) this Auger electron moves through the crystal to the surface and escapes into the vacuum. At this way it can be scattered at the atoms of the crystal.

Let us consider the electron states involved in the CVV Auger transition: a core state c (quantum numbers j_c, l_c, μ_c) and two valence states g_1, g_2 (quantum numbers $l_{1,2}, m_{1,2}, \sigma_{1,2}$). The escaping Auger electron (final state) is described by a sum over spherical waves characterized by quantum numbers $L(=l, m)$ and σ . The core holes μ_c produced in the photoemission process have different weights determined by the dipole transition probability and especially by the polarization of the light. The spinors χ_+ and χ_- contribute to the wave function of the hole state $|j_c, l_c, \mu_c\rangle$ with different weighting factors. This is a source of the spin polarization of the photoelectron. It is usual to say that the core hole has a preferred spin. The spin polarization of the hole states is transferred then to the Auger electron via matrix element M of the Auger process:

$$M(L\sigma, c|g_1, g_2) = \langle f_{L\sigma}, c|V|g_1, g_2\rangle - \langle f_{L\sigma}, c|V|g_2, g_1\rangle. \quad (1)$$

It contains the expectation value of the Coulomb interaction and the corresponding exchange integral.

The expression for the spin-polarized intensity of the Auger electrons in a direction $\mathbf{e}(\mathbf{e} = \check{\mathbf{k}} = \mathbf{r}/r, \mathbf{k} = k\mathbf{e}, k = \sqrt{E_f})$ can be written in the form

$$I_\sigma(E_f, \check{\mathbf{k}}) = \sum_{g_1 g_2} \langle M_\sigma^2 \rangle_{g_1 g_2} \int D_{g_1}(E_f + E_c - \varepsilon) D_{g_2}(\varepsilon) d\varepsilon, \quad (2)$$

where $D_g(\varepsilon)$ is the local partial density of states (DOS) (g denotes a set of quantum numbers characterizing the valence electron state) and the integration is performed over the occupied part of the valence band. This expression is obtained assuming the Auger matrix elements independent on the energy of the valence states.

Auger transition probabilities $\langle M_\sigma^2 \rangle_{g_1 g_2}$ can be expressed as

$$\langle M_\sigma^2 \rangle_{g_1 g_2} = \sum_{\mu_c} w_{\mu_c}(\vec{\varepsilon}, \hbar\omega) \left| \sum_L B_{L\sigma}(\check{\mathbf{k}}) M(L\sigma, c|g_1, g_2) \right|^2. \quad (3)$$

$w_{\mu_c}(\vec{\varepsilon}, \hbar\omega)$ is the photoionization probability for the electron state μ_c in the core shell c . It depends on the polarization $\vec{\varepsilon}$ and the energy $\hbar\omega$ of incoming photons. $B_{L\sigma}(\mathbf{k})$ is the scattering path operator. It is the same expression that describes the electron scattering in low-energy electron diffraction and photoelectron diffraction.¹⁴⁻¹⁸ It contains the expressions for the direct wave, as well as the single and the multiple scattering contributions. The effect of the electron diffraction on the Auger electrons depends also on the position \mathbf{R} of the atom emitting the Auger electron in the crystal lattice with respect to the surface. Thus, B depends on \mathbf{R} and the Auger intensity is a sum over contributions (2) for different sites \mathbf{R} .

In order to obtain the integral intensity of the considered CVV transition we have to integrate the spectral intensity (2) over the region of Auger-electron energies E_f . This gives

$$I_\sigma(\check{\mathbf{k}}) = \int I_\sigma(E_f, \check{\mathbf{k}}) dE_f = \sum_{g_1 g_2} n_{g_1} n_{g_2} \langle M_\sigma^2 \rangle_{g_1 g_2}, \quad (4)$$

where n_g is the occupation number for the corresponding valence subband. The spin-polarization of the Auger electrons is obtained from the calculated spin-polarized intensities (2) as

$$P_{\text{AE}} = \frac{I_\uparrow - I_\downarrow}{I_\uparrow + I_\downarrow}. \quad (5)$$

For the integral spin polarization the corresponding integral intensities (4) should be inserted into expression (5).

For our calculations we consider a geometry similar to that used in the experiment of Stoppmanns *et al.*,¹⁰ where the K $M_{2,3}VV$ spectra have been measured. Auger-electron emission was excited from the surface of thick potassium layers by photoionization with the circularly polarized radiation of positive helicity having the energy varied in the range 12–24 eV. The experimental data were obtained for the normal incident light and electron emission within an acceptance cone of $\pm 5^\circ$ around the surface normal. According to this experimental setup in the calculations the axis of quantization was chosen parallel to the photon wave vector, thus opposite to the surface normal.

The experimental K MVV spectra presented in Refs. 10 and 11 could not be resolved in M_2VV and M_3VV contributions due to the small value of the spin-orbit splitting of the $3p_{1/2}$ and $3p_{3/2}$ levels (equal to 0.27 eV as compared with the 2-eV width of the Auger peak). We have calculated both Auger spectra, and the superposition of M_2VV and M_3VV spectra taking into account the difference in the binding energies of the $3p$ sublevels has been considered as a final result for comparison with the experiment. The $3p_{1/2}$ core hole has another possibility for Auger decay, namely the Coster-Kronig M_2M_3V transition. This core-hole decay is competitive with the considered M_2VV one, but it could be expected that for small spin-orbit splitting of the $3p$ sublevels the probability of the M_2M_3V transition decreases rapidly.

We simulate the potassium surface with a system of muffin-tin potentials. The spherically symmetric potentials in the atomic spheres were calculated using the Mattheiss construction.¹⁹ For the exchange and correlation part of the potential the Barth-Hedin approximation²⁰ was used. The dipole matrix elements and the Auger matrix elements were calculated using scalar relativistic wave functions. Taking into account the relaxation of electron states by the core hole the Auger matrix elements (1) were obtained using the wave functions calculated including the core-hole potential whereas for the dipole matrix elements the wave functions of the ground state were used.

In the present work we have studied Auger-electron emission provided by the direct Auger wave from the emitter in the bulk of the crystal (without scattering effects). In this case the scattering path operator has a form

$$B_{L\sigma}(\check{\mathbf{k}}) = i^{-L} Y_L(\check{\mathbf{k}}). \quad (6)$$

The calculations including processes of the Auger-electron diffraction are now in progress.

TABLE I. The photoelectron intensities (8) for the $p_{1/2}$ and $p_{3/2}$ level, respectively, for circularly polarized light with positive helicity. The axis of quantization is parallel to the photon wave vector.

μ_c	$I_{\mu\uparrow}^{\text{PE}}$	$I_{\mu\downarrow}^{\text{PE}}$	$w_\mu = I_{\mu\uparrow}^{\text{PE}} + I_{\mu\downarrow}^{\text{PE}}$	$ \alpha_{j\mu+} ^2$	$ \alpha_{j\mu-} ^2$
$\frac{1}{2}$	$\frac{1}{15} R_d ^2$	$\frac{4}{15} R_d ^2$	$\frac{1}{3} R_d ^2$	$\frac{1}{3}$	$\frac{2}{3}$
$-\frac{1}{2}$	$\frac{2}{9} R_s ^2 + \frac{2}{45} R_d ^2$	$\frac{1}{15} R_d ^2$	$\frac{2}{9} R_s ^2 + \frac{1}{9} R_d ^2$	$\frac{2}{3}$	$\frac{1}{3}$
Sum	$\frac{2}{9} R_s ^2 + \frac{1}{9} R_d ^2$	$\frac{1}{3} R_d ^2$	$\frac{2}{9} R_s ^2 + \frac{4}{9} R_d ^2$		
$\frac{3}{2}$	$\frac{2}{5} R_d ^2$		$\frac{2}{5} R_d ^2$	1	0
$\frac{1}{2}$	$\frac{2}{15} R_d ^2$	$\frac{2}{15} R_d ^2$	$\frac{4}{15} R_d ^2$	$\frac{2}{3}$	$\frac{1}{3}$
$-\frac{1}{2}$	$\frac{1}{9} R_s ^2 + \frac{1}{45} R_d ^2$	$\frac{2}{15} R_d ^2$	$\frac{1}{9} R_s ^2 + \frac{7}{45} R_d ^2$	$\frac{1}{3}$	$\frac{2}{3}$
$-\frac{3}{2}$		$\frac{1}{3} R_s ^2 + \frac{1}{15} R_d ^2$	$\frac{1}{3} R_s ^2 + \frac{1}{15} R_d ^2$	0	1
Sum	$\frac{1}{9} R_s ^2 + \frac{5}{9} R_d ^2$	$\frac{1}{3} R_s ^2 + \frac{1}{3} R_d ^2$	$\frac{4}{9} R_s ^2 + \frac{8}{9} R_d ^2$		

The local partial DOS and the occupation numbers for the valence subbands were calculated by means of the self-consistent linear muffin-tin orbital (LMTO) method^{21,22} in the atomic sphere approximation and including combined corrections. The overlapping atomic spheres had radii of 2.572 Å. The angular momentum expansion of the basis functions for valence states was performed up to $l=2$. For the calculation of the local electronic structure of atoms with a core hole the LMTO–Green-function method has been used.^{23,24}

III. CORE-HOLE POLARIZATION

If we create a core hole with circularly polarized light the core hole is spin polarized. This spin polarization is different from the spin polarization of the photoelectrons. The spin polarization of the core hole is a source of the Auger-electron spin polarization.

For example, let the core hole have a positive spin polarization and the two-hole configuration be a singlet. One could expect (using a qualitative consideration only) that the Auger-electron spin polarization should be negative, i.e., have a sign opposite that of the core hole. Indeed, if the spin-up electron falls from the valence band into the core hole, the spin-down electron is lifted to the Auger state.

However, due to the selection rules involved in the Auger transition matrix elements the Auger-electron spin polarization can be quite different from the core-hole spin polarization; even it can have equal or opposite sign. This behavior will be illustrated by discussing the $K M_{2,3} VV$ Auger transition. Especially, we will show that the spin of the Auger electron can have the same sign as the spin polarization of the core hole even if the two-hole configuration is a spin singlet $S=0$.

The $p_{1/2}, p_{3/2}$ core states have the form

$$|j1\mu\rangle = \alpha_{j\mu+} Y_{1\mu-(1/2)} \chi_+ + \alpha_{j\mu-} Y_{1\mu+(1/2)} \chi_-, \quad (7)$$

where the Y_{lm} are the spherical harmonics and χ_σ is the two-component spinor. The photoelectron intensity is given by

$$I_{\mu\sigma}^{\text{PE}} = \sum_{l,m}^{l_c \pm 1} | \langle lm\sigma | \vec{\epsilon} \cdot \mathbf{e} | j_c l_c \mu_c \rangle |^2 |R_l|^2, \quad (8)$$

where $\vec{\epsilon}$ is the photon polarization, \mathbf{e} a unit vector, and R_l the radial dipole matrix element, respectively. According to the dipole selection rules an electron from the $3p_{1/2}$ or $3p_{3/2}$ level can be excited into unoccupied s or d states above the Fermi level. Calculating the photoelectron intensities for circularly polarized light with positive helicity we get the results shown in Table I. The photoelectron spin-polarization P_{PE} and the core-hole spin polarization P_{H} are given by

$$P_{\text{PE}} = \frac{\sum_{\mu} (I_{\mu\downarrow}^{\text{PE}} - I_{\mu\uparrow}^{\text{PE}})}{\sum_{\mu} w_{\mu}}, \quad P_{\text{H}} = \frac{\sum_{\mu} w_{\mu} (\alpha_{j\mu+}^2 - \alpha_{j\mu-}^2)}{\sum_{\mu} w_{\mu}}. \quad (9)$$

Using the values of Table I we obtain for the $p_{1/2}$ level

$$P_{\text{PE}} = \frac{|R_s|^2 - |R_d|^2}{|R_s|^2 + 2|R_d|^2}, \quad P_{\text{H}} = \frac{1}{3} P_{\text{PE}} = \frac{1}{3} \frac{|R_s|^2 - |R_d|^2}{|R_s|^2 + 2|R_d|^2}, \quad (10)$$

and for the $p_{3/2}$ level,

$$P_{\text{PE}} = -\frac{1}{2} \frac{|R_s|^2 - |R_d|^2}{|R_s|^2 + 2|R_d|^2}, \quad (11)$$

$$P_{\text{H}} = \frac{5}{3} P_{\text{PE}} = -\frac{5}{6} \frac{|R_s|^2 - |R_d|^2}{|R_s|^2 + 2|R_d|^2}.$$

For the $p_{1/2}$ level the value of P_{PE} is equal to +100% or to –50% if we consider transitions only into s states or d states, respectively. In these cases the core-hole spin polarization is equal to +33.3% and to –16.7%. If the $p_{3/2}$ level is excited, for P_{PE} the corresponding values are –50% and +25%, whereas for P_{H} they are equal to –83.3% and +41.7%. If both s and d channels are taken into account P_{PE} and P_{H} vary between these extremal values.

It should be noted that the transitions to the s states and to the d states lead always to the opposite sign of the spin polarization. In the case $|R_s|^2 = |R_d|^2$ these effects are cancelled, and the core hole is not polarized. Note also that for the $p_{1/2}$ level the core-hole spin polarization is smaller than that of the photoelectron, whereas for the $p_{3/2}$ level it has a considerably higher value.

Now we discuss the Auger-electron intensity (4) and its spin polarization (5). We restrict our discussion to the case of two valence s electrons that are involved in the Auger process, thus $g_1 = |00\sigma_1\rangle$, $g_2 = |00\sigma_2\rangle$, $n_g = 1$. (The detailed calculations for this atomic model are presented below, in Sec. IV.) It follows from the Auger transition selection rules that the Auger state is a p wave $|1m\sigma\rangle$. Evaluating the matrix element (1) we get

$$M = \frac{1}{4\pi} R_{fs} R_{cs} \delta_{l,1} \{ \alpha_{j\mu+} (-1)^{\mu-(1/2)} \delta_{m,(1/2)-\mu} \\ \times (\delta_{\sigma,\sigma_1} \delta_{\sigma_2,+} - \delta_{\sigma,\sigma_2} \delta_{\sigma_1,+}) + \alpha_{j\mu-} (-1)^{\mu+(1/2)} \\ \times \delta_{m,-(1/2)-\mu} (\delta_{\sigma,\sigma_1} \delta_{\sigma_2,-} - \delta_{\sigma,\sigma_2} \delta_{\sigma_1,-}) \}, \quad (12)$$

where R_{fs} and R_{cs} are the radial parts. For normal emission only $m=0$ contributes, and Auger transitions are possible including a core state with $\mu = \pm 1/2$.

Using Eq. (12), quantities given in Table I (especially $|\alpha_{j\mu+}|^2 = |\alpha_{j\mu-}|^2$), and Eq. (3) with $B_{1m\sigma}(\mathbf{e}_z) = -i\sqrt{3/4\pi} \delta_{m,0}$ the Auger-electron intensity (4) for normal emission is given by

$$I_\sigma = \frac{3}{4\pi} \left| \frac{1}{4\pi} R_{fs} R_{cs} \right|^2 \sum_{\mu} w_{\mu} \{ 2|\alpha_{j\mu+}|^2 \\ \times \delta_{\mu,(1/2)} \delta_{\sigma,-} + 2|\alpha_{j\mu-}|^2 \delta_{\mu,-(1/2)} \delta_{\sigma,+} \}. \quad (13)$$

Let us consider the case of the photoexcitation into the s channel, i.e., $|R_d|^2 = 0$. From Table I we can see that the core holes are created in the $|\frac{1}{2}1 - \frac{1}{2}\rangle$ level or in the $|\frac{3}{2}1 - \frac{3}{2}\rangle$ and $|\frac{3}{2}1 - \frac{1}{2}\rangle$ levels. Thus in both cases only $\mu = -1/2$ contributes to the intensity (13).

For the $p_{1/2}$ core state a hole is created only in the $\mu = -1/2$ level (for $|R_d|^2 = 0$, Table I), thus the photoelectron spin polarization is +100%. The core-hole spin polarization (10) is +33.3%. It differs from 100% because a spin-down part χ_- is also involved in the $\mu = -1/2$ wave function (7). From Eq. (13) we get $I_1 = 0$, thus +100% spin polarization of the Auger electron. The spin polarization of the core hole and the spin polarization of the Auger electron have the same sign. The positive spin polarization +33.3% of the core hole is determined by $\alpha_{1/2-(1/2)+}^2 = 2/3 > \alpha_{1/2-(1/2)-}^2 = 1/3$ (Table I). But due to the selection rules for the Auger transition only the term $\alpha_{1/2-(1/2)-} Y_{10} \chi_-$ of Eq. (7) can contribute to the Auger transition, thus an electron with spin down (the opposite of the core-hole polarization!) goes into the core hole and the spin-up electron is excited as the escaping Auger electron.

For the $p_{3/2}$ state the core hole can be created in the $\mu = -3/2$ or in the $\mu = -1/2$ level. In the Auger intensity (13) the term $\alpha_{3/2-(1/2)-} Y_{10} \chi_-$ is involved, which has the same spin polarization as the core hole (P_H is mainly determined

by $\alpha_{3/2-(3/2)-} Y_{1-1} \chi_-$). Thus, in this case the positive spin polarization of the Auger electron is opposite to the spin polarization of the core hole.

Summarizing we find that photoelectron spin polarization, core-hole spin polarization, and Auger-electron spin polarization are quite different quantities, and detailed consideration of electron-state quantum numbers and selection rules is required to estimate the Auger-electron spin polarization qualitatively. Nevertheless, the following discussion will show that in many cases the Auger-electron spin polarization is opposite to the core-hole spin polarization.

IV. ATOMIC MODEL INCLUDING MATRIX ELEMENTS

We begin our considerations with the so-called atomic model as it was qualitatively discussed in Ref. 10. One K atom in the bulk of potassium metal is considered with a potential equal to the crystal muffin-tin potential of K in the atomic sphere. After the photoexcitation process the atom has a core hole. In the atomic model the screening cloud is described by an additional s electron. Thus the valence configuration is s^2 and the Auger transition creates two holes in the $4s$ level.

As a first step of the Auger process we consider the primary photoexcitation of the K $3p_{1/2}$ and $3p_{3/2}$ level by the circularly polarized photon with positive helicity. The probability $w_{\mu_c}(\vec{\epsilon}, \hbar\omega)$ for this transition is determined by the square of the dipole matrix element [see Eq. (8) and Table I]. It depends on the energy of the incoming photon due to the energy dependence of the radial matrix elements. This energy dependence is presented in Fig. 1(a) and is quite different for the transitions into the s and into the d states. Whereas just above the Fermi energy of bulk K the transitions into s states have considerably higher probability, the transitions into d states dominate at higher energies. Note that this result could be obtained even without the band-structure calculation for the unoccupied electron states above the Fermi level. Continuum d wave functions obtained as a solution of the Schrödinger equation for a single muffin-tin potential show increasing amplitude in the intra-atomic region for energies close to the d resonance. This causes increasing transition probabilities from the core levels into continuum d states.

The contributions to the probability $w_{\mu_c}(\vec{\epsilon}, \hbar\omega)$ are given in Table I. The values are determined by the different factors at the spinors χ_+ and χ_- in the core states $|j_c, l_c, \mu_c\rangle$. The transition into s and d states contributes with different weight for separate core states μ_c . Using the radial dipole matrix elements of Fig. 1(a) we get an energy dependence of w_{μ_c} as shown (for the $3p_{3/2}$ level) in Fig. 1(b). For $\mu_c = 3/2$ and $1/2$ the energy dependence is determined by $|R_d|^2$. $|R_s|^2$ contributes only for $\mu_c = -3/2$ and $-1/2$. From Table I it can be seen that $w_{\mu_c} = w_{-\mu_c}$ holds for $|R_d|^2 = |R_s|^2$. But, despite the large factor of $|R_s|^2$ for $\mu_c = -3/2$ the contribution of $|R_d|^2$ dominates for energies around 4 eV.

The values of w_{μ_c} for the $3p_{1/2}$ level have qualitatively the same behavior. At small energies, where the photoelectron is excited predominantly into s states, the transition probability is determined by $\mu_c = -1/2$, whereas around 4

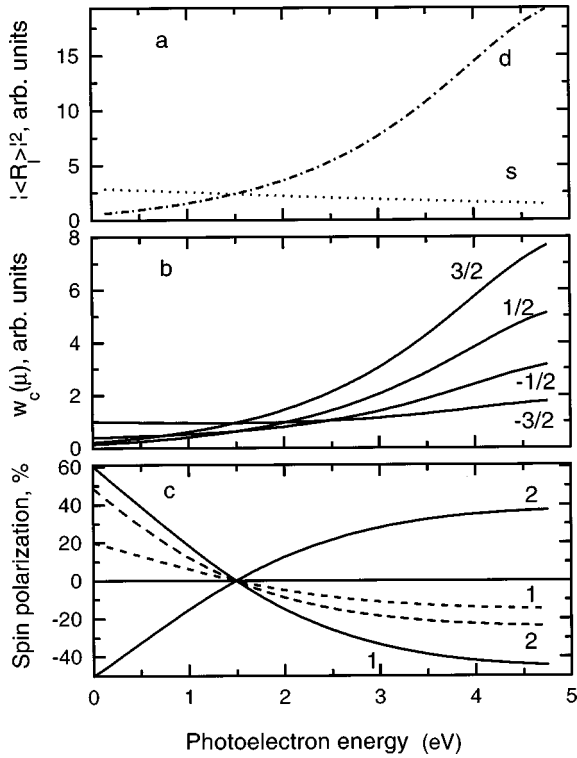


FIG. 1. (a) Squared radial dipole matrix elements for the photoexcitation of an electron from the K $3p$ core level into the unoccupied s (dotted line) and d states (dot-dashed line), (b) excitation probabilities for sublevels μ of the $3p_{3/2}$ level, and (c) spin polarization of the core hole (dashed line) and of the Auger electron (solid line) vs the photoelectron energy (measured with respect to the Fermi level). Curves (1) belong to the M_2VV transition and (2) to the M_3VV transition; only the (ss) two-hole configuration in the final state is taken into account.

eV the transitions from the state with $\mu_c = 1/2$ have much higher probability due to the large value of $|R_d|^2$.

If we consider transitions from the K $3p$ levels into s and d states separately, the core-hole spin polarization P_H (10,11) does not depend on the energy and has the values discussed in Sec. III. Taking into account both excitation channels and the energy dependence of the radial matrix elements we get an energy dependence of the core-hole spin polarization P_H as shown in Fig. 1(c). It varies from -50.2% at the threshold to 37.1% at 4.75 eV above the Fermi level for the photoexcitation of the $3p_{3/2}$ state. For the $3p_{1/2}$ level the corresponding values are equal to 20.1% and -14.8% , respectively.

The spin polarization of the core-hole state causes the spin polarization of the Auger electron P_{AE} [Eq. (5)]. Its values are modified due to the different energy dependences of the Auger transition matrix elements and the dipole matrix elements, respectively, for all quantum numbers μ_c . But in the atomic model for all energies under consideration P_{AE} has a sign that is equal to that of the core-hole spin polarization for the M_2VV transition and is the opposite of that for the M_3VV transition. That means in the atomic model P_{AE} has the same sign for both transitions.

Thus, using the simple atomic model we obtain for the M_3VV transitions the spin polarization of the Auger electron to have the value of 48.6% just above the excitation thresh-

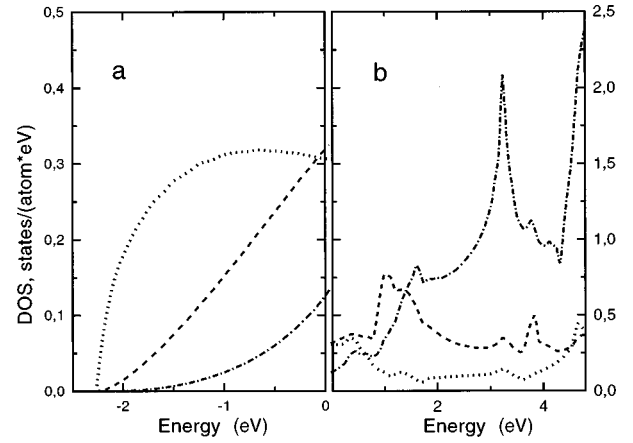


FIG. 2. Partial s (dotted line), p (dashed line), and d contributions (dot-dashed line) to the DOS in the K valence band: (a) occupied electron states, and (b) unoccupied states. Note the different scales below and above the Fermi level.

old of the K $3p_{3/2}$ level; then this value decrease with increasing photon energy to zero at 1.5 eV and to -23.9% at 4.75 eV. This behavior qualitatively agrees with the experiment;¹⁰ the energy point where the spin polarization changes sign is also very close to the measured data. However, the absolute values of the Auger-electron spin polarizations in both energy regions (where they are positive and negative) are overestimated. Moreover, if we take into account the contributions from M_2VV transitions (which provide a spin-polarization of 60.3% at threshold and of -44.5% at 4.75 eV), the overestimation becomes more considerable. Thus, we have to improve the theoretical model taking into account the valence-band structure of the K metal.

V. VALENCE-BAND STRUCTURE

In order to take into account a realistic valence-band structure of K metal we have performed self-consistent band-structure calculations by means of the LMTO method.

In contrast to a free K atom having one valence electron in the spherically symmetric s state, in the crystal the valence states are described by the Bloch function, which can be expanded locally at the atomic site in terms of angular momentum. Due to the nonspherical surroundings of the atom the contributions with $l > 0$ appear even for alkali metals. For the K metal from the decomposition of the calculated band states within the atomic sphere we get the valence electron configuration $s^{0.612}p^{0.315}d^{0.073}$. Therefore for the calculation of the Auger-electron intensities at least the contributions from the electron states of p symmetry should be taken into account.

The energy distribution of the valence electron states in potassium is shown in Fig. 2. The occupied electron states have mostly s symmetry. The p and d contributions are negligible at the bottom of the valence band; however, they increase rapidly with increasing energy, and at the Fermi level these contributions are comparable with that of s symmetry. Just above the Fermi level the p and s densities of states have higher values, but at energies above 1.5 eV d states dominate.

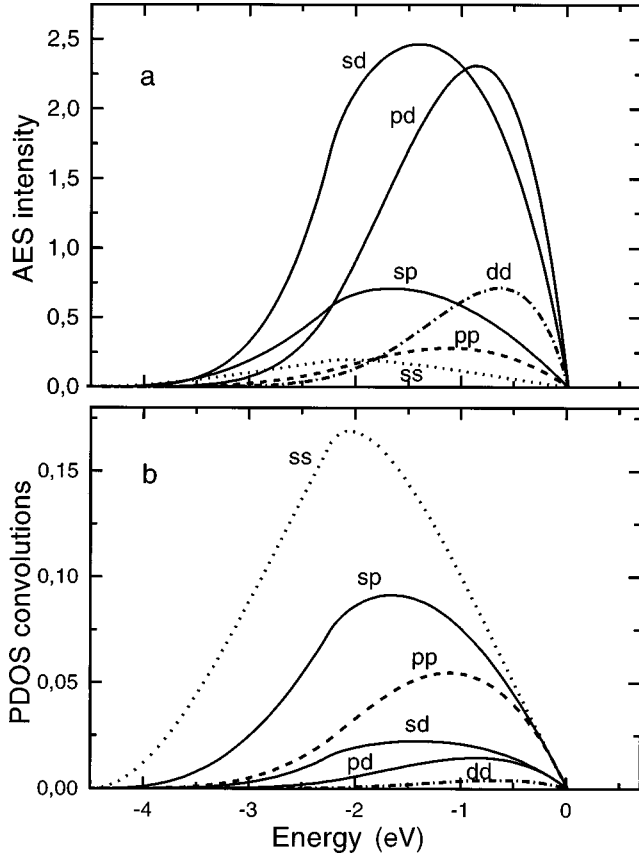


FIG. 3. Contributions of different two-hole configurations to the intensity of the M_3VV spectrum (a) and to the DOS convolution (b) for the photoelectron energy 1.5 eV.

If we consider the atom with a core hole (initial state for the Auger process) as an impurity site and perform self-consistent electronic-structure calculations for this point defect in a crystal, this results in, for the impurity valence configuration, $s^{1.062}p^{0.628}d^{0.278}$. It can be seen that the core hole is almost completely screened by the additional electronic charge transferred to the atomic sphere from the surrounding atoms. It should be noted that due to the screening the occupation numbers are significantly increased for all l states considered and we could not conclude predominantly s or p screening as has been done for Mg in Ref. 26. Note especially the increased occupation number for valence d -states due to the transferred screening charge.

In order to describe the shape of the K $M_{2,3}VV$ spectrum we have to construct self-convolutions of a partial density of states (DOS) [see expression (2)]. According to the final state rule²⁵ the valence DOS in the final state of the Auger process should be used, i.e., the valence band containing two final holes. However, the valence hole states in K metal are delocalized and do not perturb the energy distribution of the valence electrons. Thus the ground-state DOS given in Fig. 2(a) could be used for the calculation of self-convolutions. But we have to rescale them according to the impurity valence configuration. The results are shown in Fig. 3(b).

In our Auger intensity calculations for the $M_{2,3}VV$ spectrum there are contributions from the Auger transitions that create in the final-state (ss), (sp), (pp), (sd), (pd), and (dd) two-hole configuration in the valence band. These contributions to the Auger spectrum are shown in Fig. 3(a) for

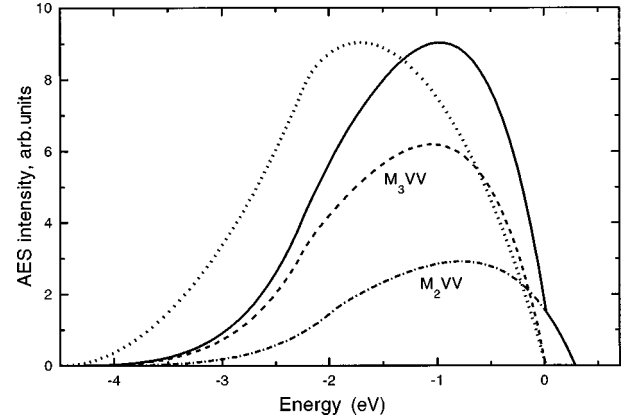


FIG. 4. Calculated Auger line profile for the photoelectron energy 1.5 eV (solid line), and the contributions from M_2VV (dot-dashed line) and M_3VV (dashed line) transitions. For comparison the profile of DOS convolution (dotted line) is shown. Energy zero was chosen at the top of the M_3VV spectrum.

the photon energy lifting the photoelectron to 1.5 eV above the Fermi level [the case of disappearing spin polarization of Auger electrons in the atomic model, see Fig. 1(c)]. The dominant contributions to the Auger intensity arise from the (sd) and (pd) two-hole states due to their higher values of transition matrix elements. Even the contribution of the (dd) configuration is of the same order of magnitude as that of the (sp) configuration in spite of the smaller occupation number of valence d states in comparison to the s and p states. It is simple to realize the role of the transition matrix elements in the formation of the Auger spectrum if we compare the contributions to the spectral intensity with self-convolutions of the partial DOS in Fig. 3(b).

The theoretical results obtained in Ref. 27 for alkali and other simple metals show that for core-valence-valence Auger decay of the initial p core hole the processes creating an (sp) two-hole final state have the maximal probability. Indeed, in our calculations the (sp) contribution would be maximal if we would not take into account the d component of the valence wave function (in Ref. 27 the d states have not been involved in the calculations). But, due to the high values of the Auger transition matrix elements for final two-hole configurations containing d states, (sd), (pd), and (dd) contributions become very important.

This can be seen in Fig. 4, which shows the calculated K $M_{2,3}VV$ spectrum. The valence d states in K are significant in the upper half of the valence band. This leads to the fact that the energy distribution of the total Auger intensity differs from the shape of the sum of partial DOS convolutions (dotted line in Fig. 4), which is determined mainly by the s and p states. Therefore the maximum of the K $M_{2,3}VV$ spectrum is shifted to higher energies and the width decreases as compared to the DOS convolution. This calculated shape of the spectral line agrees well with the experiment¹¹ where the maximal value was obtained at the energy 1 eV under the upper edge and the width was about 2 eV.

The spin polarization (5) of the Auger electrons is discussed for the energy-integrated intensity (4) for normal emission (see Sec. II). The spin polarization (5) calculated for the separate terms in the sum of the expression (4) for each combination g_1, g_2 is presented in Fig. 5 for different

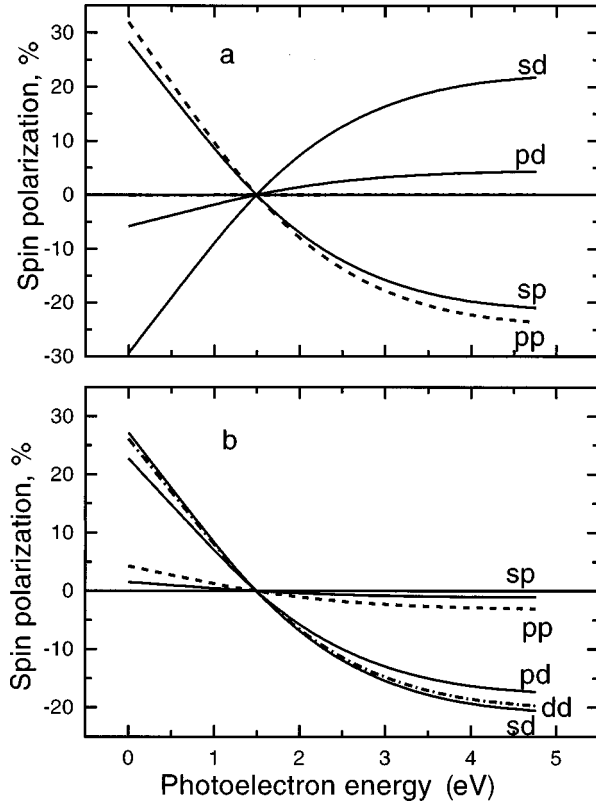


FIG. 5. The spin polarization contributions of different two-hole configurations in the direct Auger wave for M_2VV (a) and M_3VV (b) transitions vs the photoelectron energy. The spin polarization for the (ss) configuration is shown in Fig. 1(c). The dd contribution in (a) is not shown due to insignificant values of the spin polarization. Results are without scattering contributions.

photoelectron energies. The spin polarization of the total Auger flux is determined by the most intense (sd) and (pd) contributions. In the M_2VV [Fig. 5(a)] spectrum these contributions have the spin polarization of opposite sign in comparison to the (ss), (sp), and (pp) contributions. Auger transitions creating the (sd) two-hole configuration provide highly polarized Auger electrons, whereas the (pd) configuration causes the spin polarization of about $\pm 5\%$ and Auger electrons corresponding to transitions into (dd) two-hole configuration are practically nonpolarized.

In the case of the M_3VV [Fig. 5(b)] spectrum all contributions have the same qualitative behavior of the spin polarization (from positive to negative values with increasing energy). The differences in the spin polarization for the configurations containing d states are small.

The L components of the outgoing Auger wave are determined by the selection rules. In order to estimate the weight of each component for the specific Auger transition we have calculated intensity and spin polarization of the Auger emission if only one partial contribution of the Auger wave is taken into account [It means that only one term is taken into account in the sum over L in the expression (3)]. The results are summarized in Table II. It can be seen, for example, that for the (pd) two-hole configuration the outgoing d wave has the highest intensity whereas the *pure* contributions of s and g waves are very small. Note, that in the case of the (sd) configuration the most intense contribution to the M_2VV

spectrum is provided by the outgoing p wave, but the f wave dominates over the p wave for the M_3VV transition. However, it should be pointed out that the total intensity of the Auger emission is not equal to the sum of the *pure* contributions of the outgoing partial waves given in Table II due to the interference between different waves. The interference contributions appear from the square of the sum over L [see Eq. (3)] and could affect essentially the value of the Auger flux spin polarization (especially if the interference terms for spin-up and spin-down states of the Auger electron have different sign). In the case of noticeable contributions from the interference terms to the total intensity the value of the Auger-electron spin polarization cannot be deduced simply from the *pure* partial contributions presented in Table II. For example, if in the case of the (pd) two-hole configuration for the M_2VV transition the small *pure* contributions from outgoing s and g waves are neglected and we take into account the d wave only, the calculations give a wrong sign of the Auger-electron spin polarization for this two-hole configuration.

From the total intensities we can find according to Eq. (5) the spin polarization of both considered Auger spectra. In the energy region from 0 to 4.75 eV (note that the ‘‘energy’’ means here the energy of the photoelectron state above the Fermi level) the spin polarization varies between -5.9% and $+4.4\%$ for the M_2VV spectrum and between $+22.2\%$ and -16.4% for the M_3VV one. It should be pointed out that in both cases the spin polarization of the Auger electrons has a sign opposite to that of the corresponding core hole.

For comparison with the experimental data we have to overlap the calculated Auger intensities for M_2VV and M_3VV spectra taking into account that the photoionization threshold for the $3p_{1/2}$ level lies at higher photon energies due to the spin-orbit splitting of the K $3p$ level of 0.27 eV. As can be seen from Fig. 6, the calculated results are in good quantitative agreement with the experiment, especially for the low-energy side of the considered energy region and for the position of vanishing spin polarization. The total spin polarization of the K $M_{2,3}VV$ spectrum starts with 22.2% at the $3p_{3/2}$ excitation threshold, falls to 11% at the energy where M_2VV transition is switching on, then decreases to zero at 1.5 eV (the position of this point is determined only by the condition $|R_d|^2 = |R_s|^2$ and does not depend on other factors that determine the Auger process). For higher energies the spin polarization is negative, the calculated results have, however, to some extent higher absolute values than experimental ones: about -5% in the experiment and -9.7% in the calculations at energy 4.75 eV. Possible causes for these deviations are discussed below.

VI. CONCLUSIONS

We have performed the calculations of the K $M_{2,3}VV$ spectra taking into account the spin-dependent Auger transition matrix elements and the partial electron-state configuration in the valence band. It should be noted that the independent particle model used in the present calculations provides reasonable results even for the region of the excitation energies that is usually considered as a region of the resonant Auger processes. It seems that the strong screening of the core hole in metals almost removes the difference in the

TABLE II. Intensity I (in arb. units) and spin polarization P (in %) of the partial direct Auger waves for different two-hole configurations g_1, g_2 in the K $M_{2,3}VV$ spectrum. Two photoelectron energies are considered.

g_1, g_2	Auger wave	M_2VV				M_3VV			
		$E=0$ eV		$E=4.75$ eV		$E=0$ eV		$E=4.75$ eV	
		I	P	I	P	I	P	I	P
(ss)	p	0.15	60.3	1.50	-44.5	0.20	48.7	3.10	-23.9
(sp)	s	0.28	-2.0	2.83	1.5	0.59	4.5	5.96	-3.3
	d	0.15	7.7	1.47	-5.7	0.25	18.9	3.07	-11.7
	$s+d$	0.42	28.3	4.31	-20.9	0.87	1.5	9.08	-1.1
(pp)	p	0.13	12.1	1.30	-8.9	0.29	4.0	2.77	-3.2
	f	0.02	12.0	0.19	-8.9	0.03	49.8	0.38	-32.0
	$p+f$	0.15	31.9	1.48	-23.6	0.30	4.2	3.09	-3.0
(sd)	p	1.19	-4.9	12.08	3.6	0.27	42.2	3.11	-27.1
	f	0.15	10.3	1.55	-7.6	2.45	20.3	25.57	-14.5
	$p+f$	1.35	-29.4	13.6	21.7	2.93	27.2	29.07	-20.5
(pd)	s	0.03	-6.6	0.38	4.9	0.08	16.3	0.81	-12.1
	d	0.96	4.1	9.68	-3.0	2.03	21.2	20.48	-15.7
	g	0.004	6.9	0.04	-5.1	0.006	39.8	0.07	-26.1
	$s+d$	0.99	-1.5	10.05	1.1	2.12	22.1	21.32	-16.5
	$s+d+g$	1.00	-5.9	10.1	4.3	2.18	22.7	21.48	-17.3
(dd)	p	0.004	19.0	0.04	-14.1	0.01	1.5	0.10	-1.1
	f	0.26	2.7	2.63	-2.0	0.53	26.3	5.36	-19.5
	h	0.0001	6.7	0.001	-4.9	0.0001	49.8	0.001	-32.9
	$p+f$	0.26	1.3	2.68	-0.94	0.55	25.9	5.46	-19.4
	$p+f+h$	0.26	-0.08	2.68	0.06	0.55	26.1	5.47	-19.7

initial state of the emitter for the resonant and normal excitation.

It has been shown that taking into account the band structure in the K metal is very important for an accurate theoretical description of the Auger-electron intensity and spin polarization. Due to the high Auger transition probabilities the processes that create the final (sd) and (pd) two-hole states

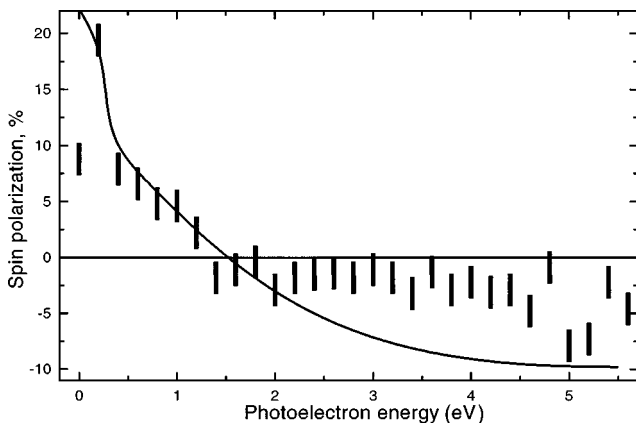


FIG. 6. Comparison of the calculated spin polarization of the K $M_{2,3}VV$ spectrum (solid line) with the experimental results (Ref. 10) (vertical bars).

are dominating for the formation of the parameters of the Auger emission. The processes creating two-hole configurations other than (ss) lead to the Auger emission with a smaller value of spin polarization. As a result we have obtained decreased values of the total spin polarization of the Auger electrons as compared to the atomic model.

It is well known from photoelectron diffraction^{28,29} that the electron scattering affects the spin polarization. Therefore, Auger-electron diffraction should be taken into account for the calculation of the spin-polarized Auger-electron emission even in the case of nonpolarized scatterers in the crystal if the Auger selection rules allow the outgoing Auger waves with different quantum numbers l . This does not appear in the atomic model as mentioned in Ref. 10. In this case according to the Auger selection rules there is only a p wave outgoing from the emitter, and the diffraction of this wave at the surrounding atoms will not change the ratio of spin-up and spin-down intensities. On the contrary, for other two-hole configurations there are direct Auger waves of different symmetry and, consequently, of different partial spin polarization. In this case the Auger electron diffraction will change the contributions of different waves to the intensity in the measured direction of the Auger emission, and this can have an effect on the spin polarization of outgoing Auger electrons. These scattering processes will be considered in a forthcoming work.

The theoretical model used in the present work describes quantitatively the experimental results obtained in Ref. 10. It should be pointed out that it is possible to significantly improve on the calculated values as compared to those provided by the atomic model. For example, whereas the atomic model gives a spin polarization of the Auger electrons of about 50% at the threshold, taking into account the electron band structure in the crystal decreases this value by factor 2.5. Our investigations confirm the ideas discussed in Ref. 10 that the spin polarization of the K M_3VV Auger electrons reflects the symmetry of unoccupied electron states above the Fermi level at the energy reached in the primary photoexcitation. The position of the energy point where the spin polarization changes its sign, especially, is determined accurately within the atomic model and is not influenced by taking into account the band structure and scattering effects.

Some deviations of the calculated results from the experimental ones could be explained by approximations used in the theoretical model. Especially, in the considered reso-

nance energy region there are contributions to the spectral intensity from the photoelectrons that are directly excited from the valence band. For the excitation energies near the $3p_{3/2}$ threshold the valence photoelectron spectrum overlaps the $M_{2,3}VV$ Auger-electron spectrum. The intensity of the M_2VV spectrum could be reduced by the existence of the competitive Coster-Kronig transition, as it was mentioned above. The Coster-Kronig transition could also change to some extent the $3p_{3/2}$ core-hole spin polarization. All these processes require an additional detail consideration and could be a subject of further theoretical investigations.

ACKNOWLEDGMENTS

We are indebted to Dr. N. Müller for stimulating discussions. This work was supported by the German Federal Ministry for Education and Research (BMBF) under Grant No. 332-4006-06 HAL 01 (8).

*Electronic address: rennert@physik.uni-halle.de

¹D. E. Ramaker, Crit. Rev. Solid State Mater. Sci. **17**, 211 (1991).

²P. Weightman, J. Electron Spectrosc. Relat. Phenom. **68**, 127 (1994).

³D. E. Ramaker, R. A. Fry, and Y. U. Idzerda, J. Electron Spectrosc. Relat. Phenom. **72**, 169 (1995).

⁴C. M. Schneider and J. Kirschner, Crit. Rev. Solid State Mater. Sci. **20**, 179 (1995).

⁵M. Landolt, in *Polarized Electrons in Surface Physics*, edited by R. Feder (World Scientific, Singapore, 1985), Chap. 9.

⁶B. Sinković, P. D. Johnson, N. B. Brookes, A. Clarke, and N. V. Smith, Phys. Rev. Lett. **62**, 2740 (1989).

⁷B. Sinković, P. D. Johnson, N. B. Brookes, A. Clarke, and N. V. Smith, Phys. Rev. B **52**, R6955 (1995).

⁸B. Sinković, E. Shekel, and S. L. Hulbert, Phys. Rev. B **52**, R15 703 (1995).

⁹P. Fuchs, K. Totland, and M. Landolt, Phys. Rev. B **53**, 9123 (1996).

¹⁰P. Stoppmanns, R. David, N. Müller, U. Heinzmann, H. Grieb, and J. Noffke, J. Phys.: Condens. Matter **6**, 4225 (1994).

¹¹N. Müller, R. David, G. Snell, R. Kuntze, M. Drescher, N. Böwering, P. Stoppmanns, S.-W. Yu, U. Heinzmann, J. Viehhaus, U. Hergenhanh, and U. Becker, J. Electron Spectrosc. Relat. Phenom. **72**, 187 (1995).

¹²P. Rennert and Yu. Kucherenko, J. Electron Spectrosc. Relat. Phenom. **76**, 157 (1995).

¹³Yu. Kucherenko and P. Rennert, J. Phys.: Condens. Matter **9**, 5003 (1997).

¹⁴J. B. Pendry, *Low-Energy Electron Diffraction* (Academic Press, London, 1974).

¹⁵P. A. Lee and J. B. Pendry, Phys. Rev. B **11**, 2795 (1975).

¹⁶C. S. Fadley, Prog. Surf. Sci. **16**, 275 (1984).

¹⁷P. Rennert and A. Chassé, Exp. Tech. Phys. (Berlin) **35**, 27 (1987).

¹⁸O. Speder, P. Rennert, and A. Chassé, Surf. Sci. **331-333**, 1383 (1995).

¹⁹L.F. Mattheiss, Phys. Rev. **133A**, 1399 (1964); **134A**, 970 (1964).

²⁰U. von Barth and L. Hedin, J. Phys. C **5**, 1629 (1972).

²¹O. K. Andersen, Phys. Rev. B **12**, 3060 (1975).

²²H. L. Skriver, *The LMTO-Method* (Springer, Berlin, 1984).

²³O. Gunnarsson, O. Jepsen, and O. K. Andersen, Phys. Rev. B **27**, 7144 (1983).

²⁴Yu. Kucherenko and A. Perlov, J. Electron Spectrosc. Relat. Phenom. **58**, 199 (1992).

²⁵D. E. Ramaker, Phys. Rev. B **25**, 7341 (1982).

²⁶A. D. Laine, G. Cubiotti, and P. Weightman, J. Phys.: Condens. Matter **2**, 2421 (1990).

²⁷C.-O. Almbladh, A. L. Morales, and G. Grossmann, Phys. Rev. B **39**, 3489 (1989).

²⁸Ch. Roth, F. U. Hillebrecht, W. G. Park, H. B. Rose, and E. Kisker, Phys. Rev. Lett. **73**, 1963 (1994).

²⁹A. Chassé and P. Rennert, J. Phys. Chem. Solids **58**, 509 (1997).